P51 ENVIRONMENTS OF SUPERCELLULAR SATELLITE TORNADOES

Roger Edwards[1] and Andrew R. Dean
Storm Prediction Center, Norman, OK

1. BACKGROUND

A satellite tornado (ST, Edwards 2014; hereafter E14) is defined as a discrete tornadic vortex occurring under all of these conditions:

- Within a supercell (even if genesis occurs outside a mesocyclone), thus precluding nonsupercellular tornadoes (e.g., Wakimoto and Wilson 1989);
- Adjacent to a longer-lasting and/or larger, mesocyclonic, main tornado (hereafter, MT) and within the MT lifespan;
- Translating around the MT for at least part of its own lifespan, in the direction matching the MT's rotational sense—thus having a common physical, mesocyclonic influence;
- Documented as a distinct tornado, not developing as part of a multiple-vortex MT circulation, based on evidence in photographs (Fig. 1), video, mobile-radar data, and/or clear description in either *Storm Data* or other meteorological literature. STs, however, can be drawn fully into a mesocyclone and sometimes are absorbed by the MT (examples in E14; French et al. 2015).

As in E14, we acknowledge the occasionally messy spectrum of vortices of tornadic and near-tornadic intensity that occur in real-world mobile-radar scenarios, rendering some cases of potential STs difficult to segregate from MTs within the mesocyclone. Wurman and Kosiba (2014) grouped STs in with such ambiguously delineated events and termed them, "multiple vortices within broad mesocyclones/surface circulations including satellite tornadoes (MVMC)". As in E14, we attempt explicit segregation of STs via use of relatively obvious observational examples (e.g., Fig. 1). We also offer no dynamical definition for an ST other than its status as a distinct, closed vortex relative to the MT (prior to any MT merger). We also continue the E14 practice of excluding mesocyclonic "handoff" tornadoes that may exist in close proximity for the latter stage of the first and the genesis of the second, such as those labelled "binary tornado" by Fujita (1992). There are no constraints on longevity, size, rotational sense, or manner of demise of the ST (i.e., dissipation before or after merger with an MT).

E14's Fig. 1 offers a two-dimensional archetypical schematic of the ST and MT from above. Photographic examples of analyzed cases herein appear in our Fig. 1. E14 did not assess the environments of ST-producing supercells, but suggested that as an area for further study. Summary updates to ST analyses from E14 will be offered in section 2. In section 3, we follow up by applying an objectively analyzed, storm-environment dataset to a filtered ST case list, and compare results with a broader national dataset of non-ST-producing tornadic supercells spanning a similar timespan. Resulting conclusions and discussion appear in section 4.

2. TORNADO DATA and ANALYSES

E14 documented 51 STs, starting with two accompanying the "Tri-State" tornado of 18 March 1925 (Johns et al. 2013), continuing through 6 June 2018. All but seven cases occurred after 1992, indicating the influence of storm spotting and chasing, and associated photographic and video material, in the documentation of STs. In fact, storm spotters and chasers have been highly valuable contributors to the database of STs, given the often ambiguous to nonexistent ST documentation in Storm Data (E14). However, because of the lack of environmental data, all E14 cases prior to the 2003 start of the SPC storm-environment database (Schneider and Dean 2008)—also known as "surface objective analysis" or SFCOA—could not be used for the environmental portion (section 3) of this follow-up study.

E14 STs were included herein, in addition to any since discovered from their period, plus all known STs from 2014–2018. The resulting dataset (SATTOR) includes 84 STs with 56 unique MTs and breaks down as follows: 18 STs with 10 unique MTs prior to 2003, and 64 STs from 2003–2018 accompanying 46 unique MTs. Figure 2 maps the STs, colorized differently from before and after environmental information is available. Given the large role of storm observers in documenting STs, the strong juxtaposition of open land (deserts, grassland, farmland) with ST reports in Fig. 2 is not surprising. STs occurring in forested areas of Arkansas, Mississippi, southern Illinois, and Indiana all were inferred from post-event damage surveys, except for two associated with eyewitness reports from the 1925 Tri-State event (Johns et al. 2013).

For analysis of tornado-path characteristics, a subset of the final, national SPC whole-tornado data ("ONETOR", Schaefer and Edwards 1999) comprising 75 STs with 53 unique MTs from 1995–2017 was selected. This era corresponds to the essentially full nationwide deployment of the WSR-88D network, and

[1] *Corresponding author address:* Roger Edwards, Storm Prediction Center, National Weather Center, 120 Boren Blvd #2300, Norman, OK 73072; E-mail: roger.edwards@noaa.gov

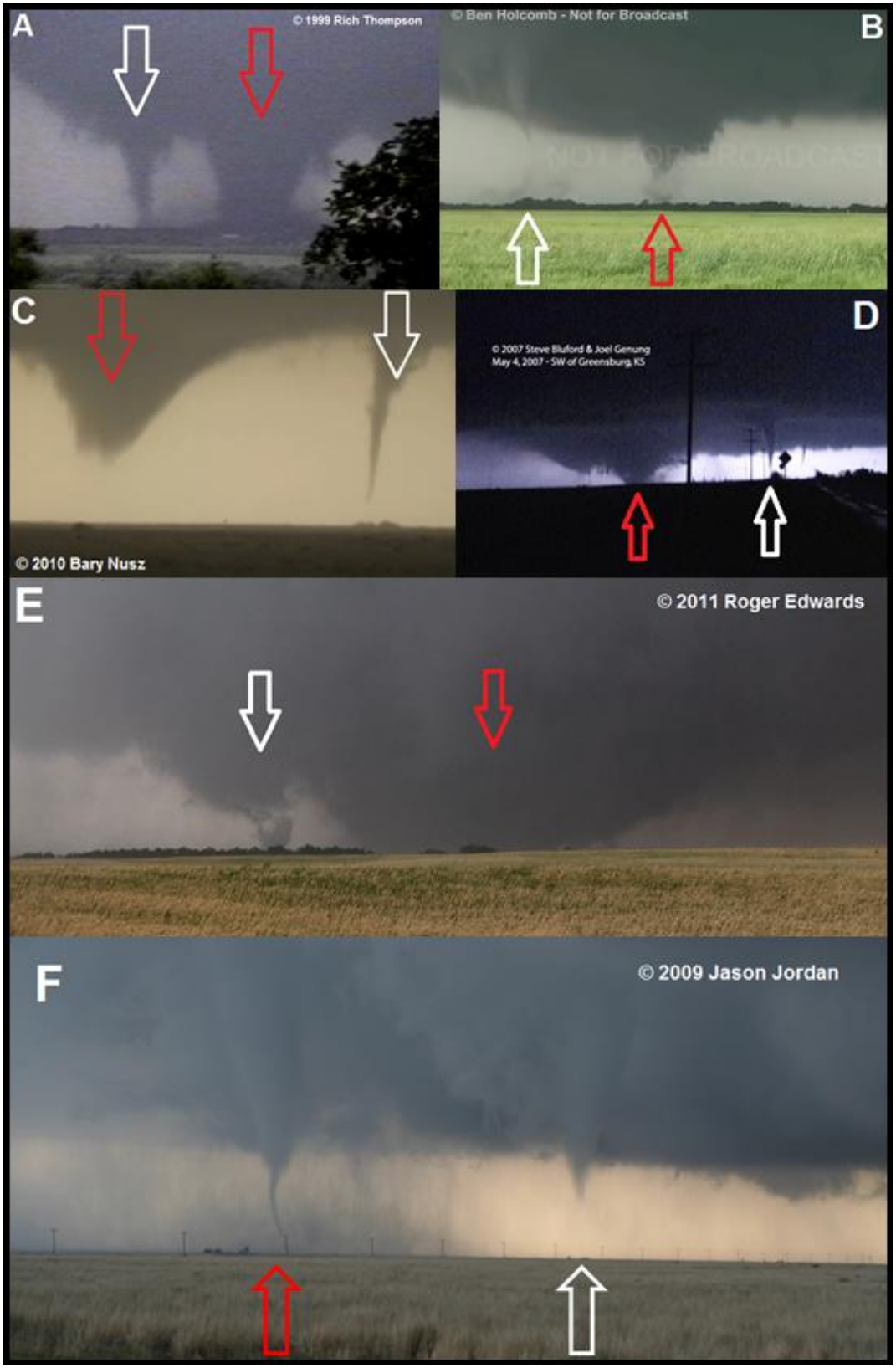

Figure 1: Photos of MTs (red arrows) and STs (white arrows) from: a) Chickasha, OK, 3 May 1999; b) Wakita, OK, 10 May 2010; c) Clayton, NM, 24 May 2010; d) Greensburg, KS, 5 May 2007 (nighttime); d) Piedmont, OK, 24 May 2011; e) South Plains, TX, 24 April 2009. Dates in UTC. A separate funnel cloud is apparent to right rear of ST in (d). *Because these are flat, two-dimensional images, MTs and STs may have been farther apart than is apparent*. Images provided by and used with permission of labeled storm observers.

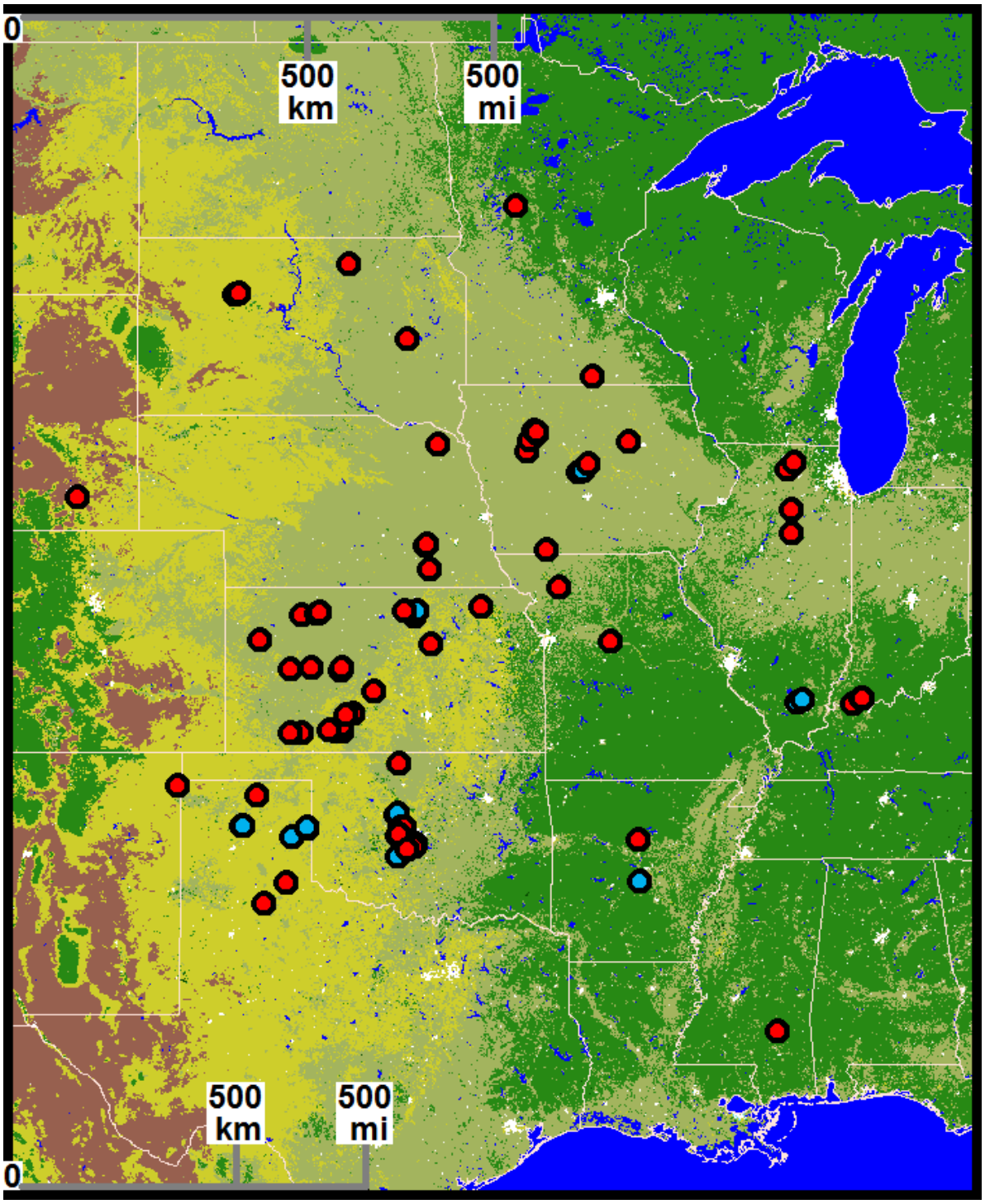

Figure 2: Map of all SATTOR entries through 2018, with those prior to SFCOA in blue and the remainder red. Due to scaling, some STs overlap. Distance scales (gray) provided for latitudes of top and bottom border of image (Mercator projection). Underlying land-use enhancement is colored as follows: water (blue), green (forested), pale green to yellow (open farmland, grassland), brick red (desert, open range, shortgrass//scrub), white (urban).

the related, relatively consistent NWS emphasis on post-event data gathering and verification. This is similar to the rationale for the period covered by the Edwards (2010) dataset of tropical cyclone tornadoes. National data for 2018 were not yet finalized as of this writing, though the specific *Storm Data* information is available regarding the 6 June 2018 ST/MT event north of Laramie, WY. As such, that event is included in the analyses.

Figure 3 shows the relative distributions of path characteristics between STs, their MTs, all ONETOR tornadoes nationally from 1995–2017, significant (EF2+ rated, per Hales 1988 convention) tornadoes from 1995–2017, and 1995–2017 violent (EF4 and

EF5) tornadoes. All but the upper whisker of ST path characteristics resides below the lower quartile of those for MTs. The below-median part the MT path characteristics overlapped the upper quartile and whisker of all significant tornadoes. The strongest interquartile overlaps between MTs and the nationwide data were with the violent tornadoes, by measures of path length, maximum path width, and the bulk parameter, "destruction potential index" (DPI; Thompson and Vescio 1998), which accounts for path length, width and F/EF-scale damage rating. The 75th and 90th percentiles of MT path width extend well beyond those for even violent tornadoes. As for STs, the distributions of their path characteristics compare well with the lower part of tornadoes as a whole (Fig. 3d), which is driven by the dominance of weak, short-lived tornadoes in the dataset, and which also is consistent with the strong concentration of STs in the weak portion of the damage-rating spectrum (Fig. 4).

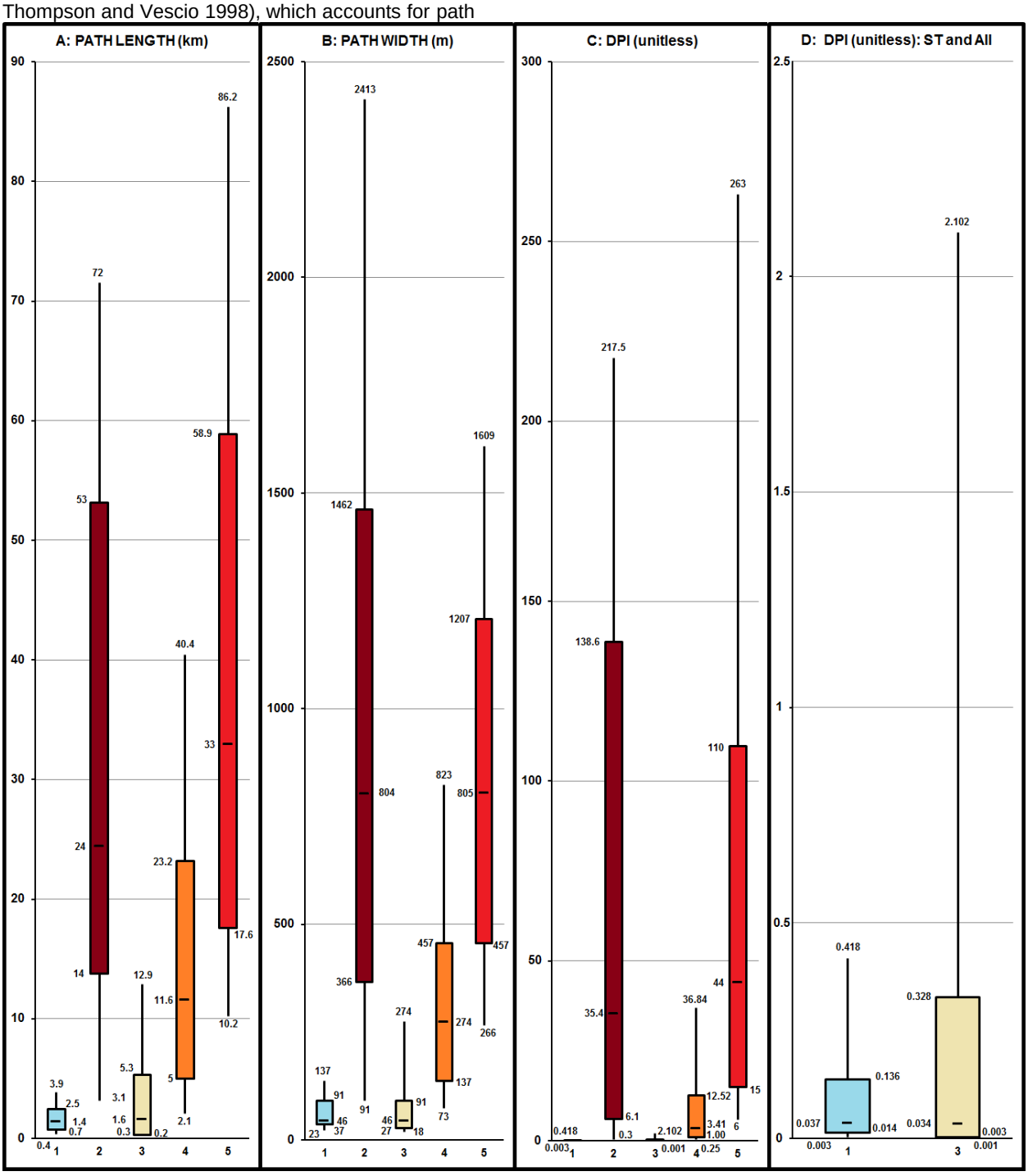

Figure 3: Boxplots for tornado-path data as labeled on the top of each panel. Boxes represent 25th to 75th percentiles. Horizontal bar is at median. Whiskers extend to 10th and 90th percentiles. Numbers on abscissa correspond to: 1) 1995–2018 STs (cyan, sample size 75); 2) 53 corresponding 1995–2018 MTs, dark red; 3) all tornadoes 1995–2017 (gold, sample size 28 447); 4) EF2+ tornadoes 1995–2017 (orange, 3099 entries); and 5) EF4–EF5 tornadoes (red, 158 events). For clearer comparison, fields (1) and (3) in panel (d) represent a zoomed version of the same fields from panel (c).

The aforementioned high-end MT bulk path characteristics, along with their preference for strong to violent parts of the damage spectrum (Fig. 4, as well as the earlier, more-preliminary E14 findings with smaller sampling), led us to hypothesize that STs occur in environments favoring strong to violent tornadoes, which is tested in the next section.

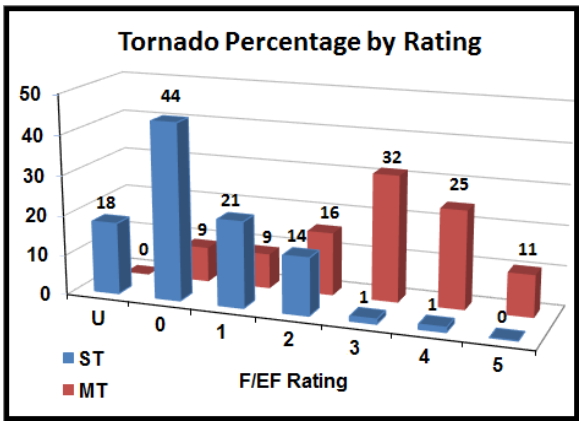

Figure 4: Bar chart representing percentage of all 1925–2018 STs (blue) and MTs (red), by F/EF-scale rating, where U stands for "unknown". Specific percentages appear above bars and may not sum to 100 because of rounding.

3. SFCOA ANALYSES and INTERPRETATION

The 2003–2018 MTs, represented by red dots in Fig. 2, were analyzed for environmental parameters present during the data hour of SFCOA (Schneider and Dean 2008) containing the recorded ST time. Table 1 summarizes the variables and their means, as compared between the MTs, all 2003–2016 tornadoes, EF2+ tornadoes only for the same period, and violent tornadoes for 2003–2016.

The relative distributions of environmental parameters between tornado classes was performed for the variables in Table 1, and nine examples appear in Fig. 5. The national tornado-environment data were obtained from a 2003–2016 update of the Smith et al. (2012) and Thompson et al. (2012) storm-mode environmental dataset, specific to tornadoes from right-moving supercells (RM) to conform to the convective mode that yields the ST schematic archetype in E14. Sample sizes of the entire national RM tornado data in Table 1 and Fig. 5 vary slightly, on the order of 10^0–10^2, due to different data availability across variables, but are maximized as follows: all tornadoes (10 244), strong tornadoes (1770) and violent tornadoes (119). The following evaluations consider Table 1 and Fig. 5 together, and the term "MT" stands as an environmental proxy for "ST" given their defined interdependence (section 1).

Distributions for kinematically derived MT variables, including those based on effective-parcel layers (Thompson et al. 2007) such as effective bulk shear-vector magnitude or effective storm-relative helicity (SRH), generally matched the significant-tornado category best (e.g., Fig. 5a,b). Fixed-layer variables such as 0–1-km SRH and 0–6-km shear-vector magnitude—both in the sense of means (Table 1), and distributions (not shown), reside between the all-tornado and significant-tornado groupings.

Table 1: Comparison of 2003–2016 means for SFCOA environmental parameters across MTs (red text), all tornadoes (gold shading), significant tornadoes (orange shading), and violent tornadoes (red shading). Variables and units (if any) are provided in alternating black and gray text. ML stands for 100-hPA-deep mixed layer; LCL is lifting condensation level, SRH is storm-relative helicity using the Bunkers et al. (2000) storm-motion technique. EFF stands for "effective" inflow parcel use, as described in Thompson et al. (2007).

VARIABLES for AVERAGES	MT	ALL	SIG	VIOL
MLCAPE (J/kg)	2395	1372	1496	2161
MLLCL (m)	1059	950	871	878
700–500-hPa LAPSE RATE (°C/km)	7.3	6.6	6.7	6.9
0–3-km LAPSE RATE (°C/km)	6.4	6.2	6.1	6.1
SURFACE RELATIVE HUMIDITY (%)	74	77	79	77
PRECIPITABLE WATER (in)	1.36	1.49	1.49	1.55
0–3-km CAPE (J/kg)	70	60	66	78
0–1-km SRH (m^2/s^2)	278	239	336	381
EFFECTIVE SRH (m^2/s^2)	346	248	354	450
0–6-km SHEAR VECTOR MAG. (kt)	51	49	56	61
EFF. SHEAR VECTOR MAG. (kt)	51	48	55	60
EFF. SUPERCELL COMP. PARM.	18	9.5	13	22
EFF. SIG. TORNADO PARM.	3.9	1.7	2.6	4.3

The only variables with little distinction of *means* among nationwide tornado classes—surface relative humidity (RH) and low-level lapse rates—were lower and higher respectively for MTs. Meanwhile MTs had a higher mean and median MLLCL than any nationwide tornado category. Greater interquartile overlap was apparent with all tornadoes, compared to strong and violent classes, on both low-level lapse rates (Fig. 5c) and MLLCL (Fig. 5f). The relative shapes and positons of the surface RH distributions (not shown) strongly resemble those for precipitable water (PW) (Fig. 5g).

Taken as a whole, these findings indicate that STs occur in somewhat drier, more deeply vertically mixed low-level environments, with slightly weaker low-level and deep shear, than the violent tornadoes they most resemble in terms of path characteristics (section 2). Given the geographic dominance of the Great Plains in MT occurrence, and higher overall LCLs for tornadoes on the Plains compared to eastern U.S. in the Thompson et al. (2003; 2007) datasets, these are not surprising results. Regardless, larger MLCAPE (Fig. 5e) was found in MT situations than in any national RM-tornado class, including a slight upward offset compared to violent tornadoes. The slightly drier environments of MTs appears to be more than counterbalanced by the influence of larger low- and middle-level lapse rates (Fig, 5c,d), associated with the Great Plains elevated mixed layer (Carlson and Ludlam 1968; Carlson et al. 1983), in yielding relatively large buoyancy for MT environments.

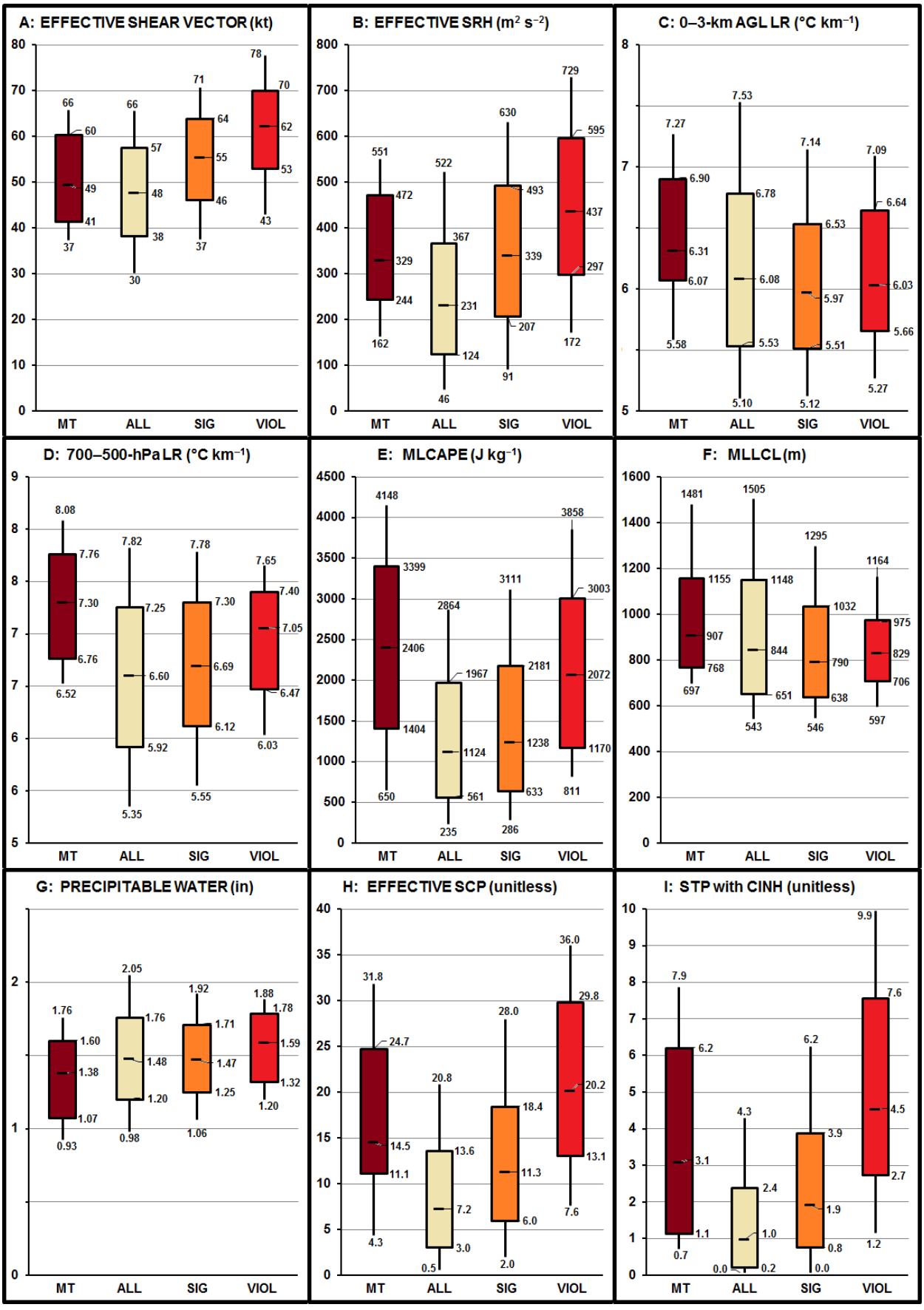

Figure 5: Box plots of distributions across MTs (2003–2018), then 2003–2016 for all tornadoes, significant tornadoes, and violent tornadoes, for nine labeled environmental parameters from Table 1. LR stands for lapse rate, SCP for supercell composite parameter, STP for significant tornado parameter. Color conventions as in Fig. 3.

Sheridan County

3 WNW Lucerne	11	1917CST						
		1920CST	0.23	25	0	0	0.00K	0.00K	Tornado (EF0)

A distinct satellite tornado formed and after several minutes merged with the first tornado which had formed two minutes earlier. A series of pictures showed two tornadoes about a quarter mile apart with one rotating around the other and finally the two merged over open fields. Thus this satellite tornado produced no damage while the first tornado went on to damage a farmhouse.

Example of Explicit Storm Data Documentation of a Satellite Tornado

A satellite tornado (left in photo) formed and rotated around the first tornado, finally merging several minutes later. Image courtesy John P. Scott.

Figure 6: Annotated screen capture of the Storm Data publication entry (NCEI 2010) for the Lucerne, KS, ST that began at 0117 UTC 12 June 2010 (1917 CST 11 June). First use of "satellite tornado" highlighted for emphasis.

The relatively maximized CAPE, combined with still-strong shear parameters, helps to drive MT composite indices such as the supercell composite and significant tornado parameters (Thompson et al, 2003; 2007) back toward the means, medians and distributions (Fig. 5e) of violent tornadoes at large, compared to the other tornado classes. To the extent the bulk indices represent RM tornadic supercell environments as a whole, this finding is more in line with the matches between MT and violent-tornado bulk path characteristics.

4. CONCLUSIONS and DISCUSSION

The first challenge in examining characteristics of STs and their environments is in their documentation. While recording of STs appears to have become more specific and precise in the overlapping era of storm-chaser proliferation, smart phones and social media, explicit documentation of STs still has been incomplete during the last decade. Ideally, STs are surveyed and mapped in a manner clearly distinguishable from the MT, consistent with their physical nature. Positive examples include the specificity of STs in the 3 May 1999 Oklahoma tornado-outbreak surveys by Speheger et al. (2002), damage-contoured survey-mapping work by R. Przybilinski for the Evansville, IN events of 6 November 2005) (Fig. 4 in E14), and illustrated *Storm Data* documentation of a Kansas ST in Fig. 6 above. Presumably, as use of the NWS Damage Assessment Toolkit (Camp et al. 2014) has become ubiquitous in U.S. tornado-damage surveys, the explicit segregation of STs should continue improving in terms of existence and precision.

Regardless, due to the relative youth of explicit ST documentation, their small, short-lived and sometimes path-overlapping nature compared to MTs, and the challenges of ST observation in situations of poor direct visibility, a thorough climatology of STs likely will remain elusive for the foreseeable future. Furthermore, the ST archetype (E14's Fig. 1) may break down in certain extreme, spectrally ambiguous and/or hybridized vortex situations such as the El Reno, OK, tornado complex of 31 May 2013 (e.g., Theim et al. 2014; Wurman et al. 2014). These statements are not meant to discourage ST classification and research, but instead to frame them in a due perspective of uncertainty: the closer that a possible ST situation conforms to the archetype, in an area of relatively good visibility, with conscientious spotters and/or sound post-event survey techniques, the more likely it will be precisely and accurately recorded as an ST in the larger body of tornado data. That uncertainty necessarily extends to the edges of ST definition as well, since tornadoes as a whole comprise a nebulously partitioned spectrum of vortex characteristics (e.g., the informal discussion by Doswell 2001).

Uncertainty also exists in tornado rating, and parameters and analyses derived therefrom, given the dependence of damage assessment on human subjectivity, the necessity of suitable damage indicators (which are less dense in open country where STs are most observed) to rate damage representatively, and the evolution of damage-assessment techniques (Edwards et al. 2013). Mobile-radar data indicate tornado intensity in general may be underrepresented by damage ratings where STs tend to be documented most: the Great Plains and open country (Alexander and Wurman 2008). Still, useful insights are emerging when examining STs, especially in the senses of known path characteristics and available environmental

information. Finally, sample-size issues (Doswell 2007) also limit the efficacy of bulk ST analysis, given their current double-digit count.

The preference of MTs to occupy the upper reaches of the tornadic size spectrum, and substantially overlapping violent tornadoes nationwide in other path and mesoscale environmental attributes (sections 1 and 2), suggest that extreme magnitudes and behaviors of vorticity fields are present in their storm-scale environments that contribute to ST formation. This idea may be worth investigating in the context of streamwise vorticity currents simulated at high resolution, one example of which was, ironically, the Orf (2017) modeling of the 24 May 2011 supercell and MT. That simulation produced EF5-equivalent winds in its tornado, successfully matching the official rating of the real MT, but without any simulated ST. In reality, that MT yielded two STs in this dataset, including the one in Fig. 1d and another observed by the lead author and by mobile radars (French et al. 2015) that apparently became about as strong as the (temporarily weakened stage of the) MT, before merging with it.

Aside from post-event surveys discussed in section 2, the degree to which eastern U.S. STs are underreported or simply do not occur is unknown. Improved damage-survey practices and emphasis on storm spotting can help to gain more insight on the truer relative distribution of STs nationwide. The vital role of chasers and spotters in documenting STs to date underscores the importance of safe storm observing in acquiring tornado information (Doswell et al. 1999), not only for real-time warning operations and post-event verification, but for research such as this. As noted in E14, safe observing practices, especially in environments already favoring strong to violent tornadoes, necessarily should include heightened awareness of visual mesocyclone behavior in looking for STs, and keeping safe distance in order to avoid being hit by the ST while fixated on the MT.

ACKNOWLEDGMENTS

These individuals contributed discussion, event information, leads, and/or photos from afield: Ed Aldrine, the late Matt Biddle, Steve Bluford, Brock Burghardt, Casey Crosbie, Scott Currens, Charles Edwards, Elke Edwards, David Ewoldt, Mike French, Joel Genung, Greg Gust, Robert Herman, Ben Holcomb, Ryan Husted, Brandon Ivey, Bob Johns, Jim LaDue, Tony Laubach, Tony Lyza, Jared Leighton, Gene Moore, Bary Nusz, Al Pietrycha, the late Ron Przybilinski, Neal Rasmussen, Bill Reid, Dan Robinson, John Robinson, John Scott, Daniel Shaw, Pat Skinner, Jeff Snyder, Doug Speheger, Jerry Straka, Skip Talbot, Rich Thompson, and Mike Umscheid. Without them, and other storm observers who provided information to local NWS offices for those events that were included in *Storm Data*, this study would not have been possible. Bryan Smith and Rich Thompson provided a supercell-specific tornado-environment dataset for our comparative analysis. Israel Jirak (SPC) performed astute review of this extended abstract.

REFERENCES

Alexander, C., and J. Wurman, 2008: Updated mobile radar climatology of supercell tornado structures and dynamics. Preprints, *24th Conf. on Severe Local Storms*, Savannah, GA, Amer. Meteor. Soc., 19.4.

Bunkers, M. J., B. A. Klimowski, J. W. Zeitler, R. L. Thompson, and M. L. Weisman, 2000: Predicting supercell motion using a new hodograph technique. *Wea. Forecasting*, **15**, 61–79.

Camp, J. P., L. P. Rothfusz, A. Anderson, D. Speheger, K. L. Ortega, and B. R. Smith, 2014: Assessing the Moore, Oklahoma (2013) tornado using the National Weather Service Damage Assessment Toolkit. *Special Symp. on Severe Local Storms: The Current State of the Science and Understanding Impacts*, Atlanta, GA, Amer. Meteor. Soc., 830.

Carlson, T. N., and F. H. Ludlam, 1968: Conditions for the occurrence of severe local storms. *Tellus*, **20**, 203–226.

——, S. G. Benjamin, G. S. Forbes, and Y. F. Li, 1983: Elevated mixed layers in the regional severe storm environment: Conceptual model and case studies. *Mon. Wea. Rev.*, 111, 1453–1473.

Doswell, C. A. III, 2001: What is a tornado? [Available online at http://www.cimms.ou.edu/~doswell/a_tornado/atornado.html.]

——, 2007: Small sample size and data quality issues illustrated using tornado occurrence data. *Electronic J. Severe Storms Meteor.*, **2** (5), 1–16.

——, A. R. Moller, and H. E. Brooks, 1999: Storm spotting and public awareness since the first tornado forecasts of 1948. *Wea. Forecasting*, **14**, 544–557.

Edwards, R., 2010: Tropical cyclone tornado records for the modernized National Weather Service era. Preprints, *25th Conf. on Severe Local Storms*, Denver, CO, Amer. Meteor. Soc., P3.1.

——, 2014: Characteristics of supercellular satellite tornadoes. Preprints, *27th Conf. on Severe Local Storms*, Madison, WI, Amer. Meteor. Soc., 17.5.

——, J. G. LaDue, J. T. Ferree, K. L. Scharfenberg, C. Maier, and W. L. Coulbourne, 2013: Tornado intensity estimation: Past, present and future. *Bull. Amer. Meteor. Soc.*, **94**, 641–653.

French, M. M., P. S. Skinner, L. J. Wicker, and H. B. Bluestein, 2015: Documenting a rare tornado merger observed in the 24 May 2011 El Reno–Piedmont, Oklahoma, supercell. *Mon. Wea. Rev.*, 143, 3025–3043.

Fujita, T. T., 1992: *Memoirs of an Effort to Unlock the Mystery of Severe Storms*. University of Chicago, 298 pp.

Hales, J. E. Jr., 1988: Improving the watch/warning program through use of significant event data. Preprints, *15th Conf. on Severe Local Storms*, Baltimore, MD, Amer. Meteor. Soc., 165–168.

Johns, R. H., D. W. Burgess, C. A Doswell III, M. S. Gilmore, J. A. Hart, and S. F. Piltz, 2013: The 1925 Tri-State tornado damage path and associated storm system: Supplemental material. *Electronic J. Severe Storms Meteor*., **8** (2), C1–C31.

NCDC, 2010: *Storm Data*. Vol. 52, no. 6, 361.

Orf, L., R. Wilhelmson, B. Lee, C. Finley, and A. Houston, 2017: Evolution of a long-track violent tornado within a simulated supercell. *Bull. Amer. Meteor. Soc.*, **98**, 45–68.

Schaefer, J. T., and R. Edwards, 1999: The SPC tornado/severe thunderstorm database. Preprints, *11th Conf. on Applied Climatology*, Dallas, TX, Amer. Meteor. Soc., 215–220.

Schneider, R. S. and A. R. Dean, 2008: A comprehensive 5-year severe storm environment climatology for the continental United States. Preprints, 24th Conf. on Severe Local Storms, Savannah, GA, Amer. Meteor. Soc., 16A.4.

Smith, B. T., R. L. Thompson, J. S. Grams, C. Broyles, and H. E. Brooks, 2012: Convective modes for significant severe thunderstorms in the contiguous United States. Part I: Storm classification and climatology. *Wea. Forecasting*, **27**, 1114–1135.

Speheger, D. A., C. A. Doswell III, and G. J. Stumpf, 2002: The tornadoes of 3 May 1999: Event verification in central Oklahoma and related issues. *Wea. Forecasting*, **17**, 362–381.

Theim, K. J., H. B. Bluestein, J. C. Snyder, and J. Houser, 2014: Rapid-scan, polarimetric, mobile, Doppler-radar observations of the formation, evolution, and structure of the El Reno tornado of 31 May 2013. Preprints, *24th Conf. on Severe Local Storms*, Madison, WI, Amer. Meteor. Soc., 13.4.

Thompson, R. L., and M. D. Vescio, 1998. The destruction potential index—A method for comparing tornado days. Preprints, *19th Conf. on Severe Local Storms*, Minneapolis, MN, Amer. Meteor. Soc., 280–282.

——, R. L., R. Edwards, J. A. Hart, K. L. Elmore, and P. M. Markowski, 2003: Close proximity soundings within supercell environments obtained from the Rapid Update Cycle. *Wea. Forecasting*, **18**, 1243–1261.

——, C. M. Mead, and R. Edwards, 2007: Effective storm-relative helicity and bulk shear in supercell thunderstorm environments. *Wea. Forecasting*, **22**, 102–115.

——, B. T. Smith, J. S. Grams, A. R. Dean, and C. Broyles, 2012: Convective modes for significant severe thunderstorms in the contiguous United States. Part II: Supercell and QLCS tornado environments. *Wea. Forecasting*, **27**, 1136–1154.

Wakimoto, R. M. and J. W. Wilson, 1989: Non-supercell tornadoes. *Mon. Wea. Rev.*, **117**, 1113–1140.

Wurman, J., K. Kosiba, P. Robinson, and T.P. Marshall, 2014: The role of multiple-vortex tornado structure in causing storm researcher fatalities. *Bull. Amer. Meteor. Soc.*, **95**, 31–45.